

A Mechanically Pumped Two-Phase Fluid Loop for Thermal Control Based on the Capillary Pumped Loop

Benjamin Furst¹, Stefano Cappucci², Takuro Daimaru³, Eric Sunada⁴
Jet Propulsion Laboratory/California Institute of Technology, Pasadena, California, 91101

A novel two-phase Mechanically Pumped Fluid Loop (MPFL) for thermal control is presented. The operating principles are outlined and results from a prototype test facility are shown. The system is a variant of the Capillary Pumped Loop (CPL) where a mechanical pump and bypass line have been added to make a pump-assisted CPL. The benefits of this design are discussed, and test results are shown that demonstrate the feasibility of the system architecture. Stable performance for heat loads between 30 W and 850 W are reported along with the capability of handling a heat flux of up to 13 W/cm². In addition, the testbed incorporates a novel planar Additively Manufactured (AM) evaporator. Preliminary test results show that the evaporator can maintain isothermality within 0.5 C for heat loads upto 100 W and within 3 C for heat loads up to 325 W.

Nomenclature

<i>NASA</i>	=	National Aeronautics and Space Administration
<i>JPL</i>	=	Jet Propulsion Laboratory
<i>MPFL</i>	=	Mechanically Pumped Fluid Loop
<i>CPL</i>	=	Capillary Pumped Loop
<i>LHP</i>	=	Loop Heat Pipe
<i>AM</i>	=	Additively Manufactured
<i>MAWP</i>	=	Max Allowable Working Pressure
<i>DMLS</i>	=	Direct Metal Laser Sintering

I. Introduction

FUTURE NASA missions will require thermal control systems that exceed the capabilities of currently available space-qualified systems. Multiple mission concepts are under development that require the dissipation of high heat fluxes, the transport of large amounts of heat long distances, and increasingly tight temperature control.¹⁻³ As always, the desired enhancements in thermal performance are sought to be made with minimal impact to resources (mass and power).

A commonly considered solution to meet these objectives is a two-phase Mechanically Pumped Fluid Loop (MPFL).⁴⁻⁷ A two-phase MPFL has the potential to combine the best elements of both passive two-phase thermal control systems and single-phase MPFL thermal control systems. Such a system could be relatively lightweight, have high thermal conductance, have the ability to handle high heat fluxes and large heat loads, and have set point temperature control and a high degree of isothermality (traits of two-phase devices). In addition it could be versatile, and easy to integrate and test (traits of single phase MPFLs).

¹ Thermal Technologist, Propulsion, Thermal, and Materials Engineering Section, 4800 Oak Grove Dr., Pasadena, CA 91109, Mail Stop 125-123.

² Thermal Engineer, Propulsion, Thermal, and Materials Engineering Section, 4800 Oak Grove Dr., Pasadena, CA 91109, Mail Stop 125-123

³ Thermal Engineer, Propulsion, Thermal, and Materials Engineering Section, 4800 Oak Grove Dr., Pasadena, CA 91109, Mail Stop 125-123

⁴ Principal Thermal Engineer, Propulsion, Thermal, and Materials Engineering Section, 4800 Oak Grove Dr., Pasadena, CA 91109, Mail Stop 125-123.

Here a two-phase MPFL is presented that attempts to incorporate all of these attributes. In the following sections the system architecture is outlined and preliminary test results from a prototype system are presented. This system was first proposed in Ref. 8 and is subsequently discussed in Refs. 9-11.

II. System Architecture

The two-phase MPFL system architecture discussed here is based on a Capillary Pumped Loop (CPL);¹² it therefore makes sense to review CPL operation. Figure 1 (left) shows a schematic of typical CPL. In this system the heat load is acquired at the evaporator and rejected at the condenser and subcooler. The fluid is transported around the circuit via capillary pumping that occurs in the evaporator. The heat load and transport length of a CPL are limited by the capillary pumping that the evaporator wick can sustain. In particular the total pressure drop in the system must be less than the available capillary pumping pressure in the wick.¹²

The two-phase MPFL considered here uses the same basic layout as a CPL, and in particular uses the same evaporator layout (i.e. a liquid and vapor channel separated by a porous wick). The primary difference is the addition of a mechanical pump and bypass line. Figure 1-right shows a schematic of the system; note the similarity to the CPL layout (Figure 1- left). In this system the mechanical pump is placed with its inlet close to the accumulator and its outlet directed towards the evaporator. The bypass line is situated in parallel with the evaporator line, such that it connects the pump outlet directly to the condenser outlet. As will be discussed later, the bypass line can also be terminated closer to the evaporator outlet to enhance certain system capabilities. The addition of the mechanical pump and bypass line significantly impact the performance of the system. The system level steady state operation mechanics are described below. The addition of the mechanical pump to the CPL architecture suggest that the system is a pump-assisted CPL. A variant of this system was first presented in.⁸

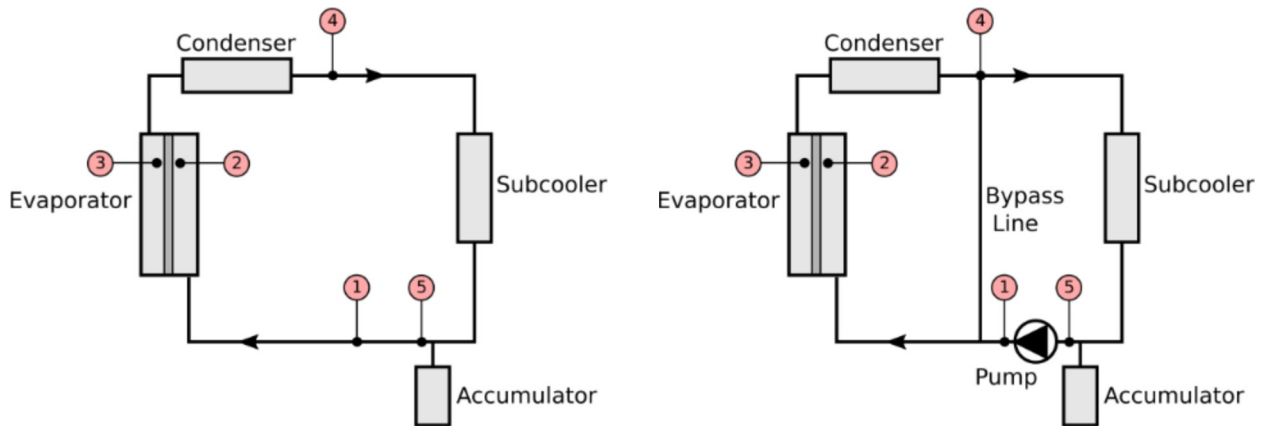


Figure 1. Schematic of a CPL (left) and the proposed two-phase MPFL (right). For a CPL (left), heat is transported from the evaporator to the condenser via fluid flow generated by capillary pumping in the evaporator. For the two-phase MPFL (right), heat is transported in a similar manner, although the capillary pumping in the evaporator is assisted by the mechanical pump. This two-phase MPFL is also referred to as a pump-assisted CPL.

A. System Operation

To understand how this two-phase MPFL architecture functions, consider a steady state nominal operating condition where: (1) a constant heat load is applied to the evaporator; (2) the pump is operating at a fixed speed; and (3) the accumulator temperature is being held at a constant temperature above the subcooler temperature. Additionally assume that the heat load is sufficient to create enough vapor to fill the vapor channels in the evaporator and the line between the evaporator and condenser, and that the wick is producing some degree of capillary pumping. This situation can be physically realized in an experimental system as is shown in section IV below.

Assuming this operating state exists, several observations can be made. (References will be made to Figure 1-right). Firstly, as in a CPL the pressure differential across the meniscus ΔP_{32} results in a higher pressure on the vapor side (location 3) and a lower pressure on the liquid side (location 2). This circumstance presents a hydrodynamic wall condition for the pump, since fluid cannot flow from a low pressure to a high pressure by hydrodynamic means.

(The mass transfer across this pressure differential is due to evaporation.) This implies that the pump is not pushing fluid through the evaporator, rather it is only pushing fluid through the bypass line. The flowrate through the evaporator is completely dictated by the heat load, as in a CPL.

To further understand the consequences of this, consider a pressure balance between points 1 and 4 in Figure 1-right:

$$\Delta P_{14} = \Delta P_{12} + \Delta P_{34} - \Delta P_{32} \quad (1)$$

Where ΔP_{14} is the pressure drop across the bypass line, $(\Delta P_{12} + \Delta P_{34})$ is the pressure drop in the evaporator line (before and after), and ΔP_{32} is the capillary pressure rise across the menisci in the wick. Eqn. 1 can be rearranged to yield:

$$\Delta P_{32} + \Delta P_{14} = \Delta P_{12} + \Delta P_{34} \quad (2)$$

Eqn. 2 shows that the pressure loss in the evaporator line and condenser $(\Delta P_{12} + \Delta P_{34})$ is balanced by the capillary pressure rise (ΔP_{32}) and the pressure loss in the bypass line (ΔP_{14}) . As noted previously, the fluid flow in the bypass line is completely provided by the mechanical pump. Therefore the pressure loss in the bypass line (ΔP_{14}) is dictated by the mechanical pump flowrate and bypass line fluid flow resistance. In this way, the mechanical pump and bypass line combination indirectly assists with the capillary pumping in the evaporator by maintaining the pressure drop across the bypass line (ΔP_{14}) . Viewed another way, the addition of the mechanical pump and bypass line allow the pressure at location 4 (Figure 2) to be controlled independently of the heat load applied to the evaporator. This means that the pressure at location 4 (Figure 2) can be reduced, effectively providing a suction pressure at the condenser outlet to help the capillary forces move fluid through the evaporator. A similar analysis and conclusions were previously presented in.^{8,9}

B. Comparison of the CPL and pump-assisted CPL

As can be seen in the previous analysis, the addition of a mechanical pump and bypass line to a CPL essentially provide additional pressure head beyond the capillary pressure to help circulate fluid around the loop. However, for a properly designed pump-assisted CPL, part of the system (the evaporator and condenser) still operate in the same manner as a CPL: There is still a liquid/vapor interface (menisci) in the wick which sustains capillary pumping, and the line between the evaporator and the condenser contains pure vapor.

In order to further distinguish the pump-assisted CPL, it will be compared to a CPL in more detail below. Note that much of what applies to a CPL in the discussion below also applies to a Loop Heat Pipe (LHP) as well.

Consider the pressure diagram of a CPL and pump-assisted CPL shown in Figure 2. This diagram shows a representative plot of pressure versus location for the CPL and pump-assisted CPL schematically shown in Figure 1-left and Figure 1-right. To facilitate the comparison, the accumulator for both systems are assumed to be at the same reference pressure.

In the CPL shown in Figure 1-left, liquid flowing from location 5 to location 2 results in a slight pressure drop; between locations 2 and 3 the liquid is evaporated and transported across the menisci in the wick. The fluid undergoes a rise in pressure that is produced by the vapor pressure and sustained by the menisci (i.e. capillary pumping). As the fluid flows from the evaporator outlet (location 3) back to the accumulator (location 5) the pressure drops are due to vapor flow in the evaporator transport line, two-phase flow in the condenser and liquid flow in the subcooler. In order to sustain proper operation, the total pressure drop of the system must be less than the available capillary pumping pressure that can be sustained by the evaporator wick.⁵

For the pump-assisted CPL, the pressure diagram references the outer circuit of Figure 1-right. In this system there is a pressure rise from locations 5 to 1 due to the mechanical pump. This is followed by a pressure drop in the liquid flowing to the evaporator (location 2). As in the CPL there is a pressure rise across the menisci in the wick from locations 2 to 3. From location 3 to 5 the pressure monotonically decreases due to vapor flow (evaporator), two-phase flow (condenser), and liquid flow (subcooler). Note that the pressure at location 4 can be independently controlled via the pressure drop across the bypass line. In the pump-assisted CPL, the available pressure head is equal to the sum of the mechanical pumping pressure and the capillary pumping pressure of the evaporator wick.

This comparison highlights the operational advantage of the pump-assisted CPL architecture. For a CPL (or LHP) the pressure drops of the system must be less than the available capillary pressure of the wick. This puts limitations on the maximum allowable heat load and transport line length, as these influence the system pressure drop. For a CPL/LHP, the system capability is completely dictated by the wick properties (pore size, permeability, etc). This limitation does not exist in the pump-assisted CPL shown here. In the pump-assisted CPL, the pressure

capability of a mechanical pump supplements the capillary pressure of the wick. The maximum heat transport capability and line length for this system are only limited by the mechanical pump. This enables the pump-assisted CPL to scale to much larger systems than are possible with a typical CPL/LHP.

While the additional pumping head of the pump-assisted CPL over a typical CPL/LHP is the most obvious advantage, there are two other benefits that are worth mentioning. The first is that the pump-assisted CPL provides the potential for much simpler integration than a CPL/LHP. A pump-assisted CPL can fairly easily accommodate mechanical fittings and line routing changes. This simplifies interfaces within the spacecraft. The second benefit is that a pump-assisted CPL can be ground tested in any orientation, as the mechanical pump can be used to negate gravity effects on the system. This is not the case with a CPL/LHP.

The pump-assisted CPL architecture presented here also shows a number of benefits over the classical two-phase MPFL design that relies on mixed flow in the evaporator.⁵ It requires no pre-heater to bring the working fluid to saturation at the evaporator inlet (instead pre-heating naturally occurs in the evaporator—as in a CPL); the region of two-phase flow is much smaller (limited only to the condenser); the pressure drop is less for a given heat load (since there is less 2-phase flow), and thus the required pumping power is less. In addition the pump-assisted CPL is more predictable, as the region of two-flow is minimized. During normal operation, most of the system lines contain single phase flow, which is very amenable to prediction. Finally, in the event of a pump failure, the pump-assisted CPL could operate as a CPL with degraded performance.

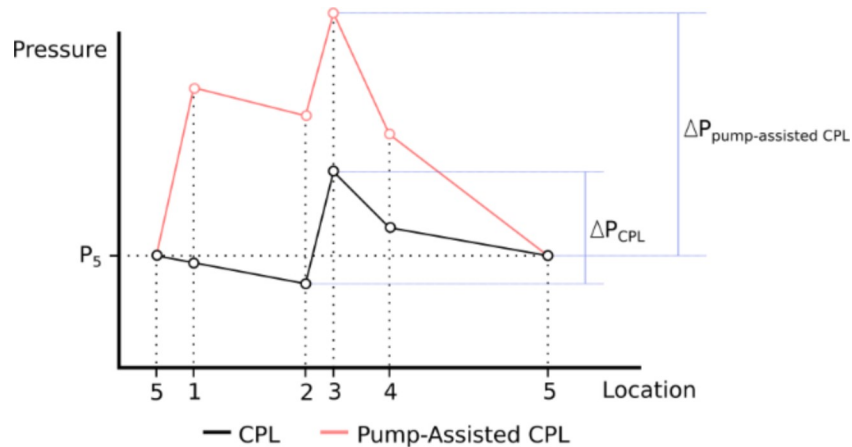


Figure 2. Pressure vs. position diagram for a CPL and pump-assisted CPL. For a CPL, the available pumping power is limited to the maximum available capillary pressure; for a pump-assisted CPL, the available pumping power is equal to the sum of the capillary and mechanical pumps. The locations referred to on the abscissa correspond to the fluid loop locations shown in Figure 1.

C. Performance limitations of the pump-assisted CPL

Some performance limitations of a pump-assisted CPL based on a simple analysis were first described in Ref. 8. These are summarized here. There are 2 basic limitations on the performance of a pump-assisted CPL that are derived from the requirement that the menisci in the wick must separate the phases. Operational failure can occur if either vapor penetrates into the liquid side of the evaporator, or if liquid penetrates into the vapor side of the evaporator. Vapor will penetration will occur when the heat load is too high and is generating more vapor than can flow out to the condenser. In this case, the pressure differential across the meniscus will overwhelm the capillary pressure that can be maintained by the meniscus. This will happen if the system does not have enough pumping potential. Conversely liquid will penetration will occur if the heat load is not high enough or there is too much mechanical pump pressure (e.g. the pressure at location 4 is too low). In this case the pressure on the liquid side of the meniscus will be higher than the pressure on the vapor side. For a given pump speed (total system flowrate) there will exist a maximum and minimum allowable heat load based on these failure mechanisms. This dynamic range depends on the properties of the wick, and a smaller pore size will have a larger dynamic range. A previous trade study showed that with proper design, a pump-assisted CPL could have operating ranges of at least 1 kW.⁹ Two possible ways to circumvent this issue (and increase the operating range) are to either use a variable speed pump or incorporate an adjustable valve in the bypass line. Another potential method is move the terminus of the bypass line

closer to the evaporator. This reduces the pressure drop that is compensated for by capillary pumping and thus increases the dynamic range.

III. A Pump-Assisted CPL Testbed

A two-phase MPFL with the pump-assisted CPL architecture described above was built and tested. Knowledge from prior testing informed the system design.^{8,10} The working fluid was selected to be ammonia following a comprehensive trade study.⁹ In addition to testing out this new architecture, the testbed was used to try a novel Additively Manufactured (AM) planar CPL type evaporator. The evaporator is briefly discussed below; for a more in depth discussion see Refs. 10,11. Further details of the testbed are discussed below.

D. Testbed Design

A schematic of the pump-assisted CPL testbed is shown in Figure 3. The primary functional components of the system are the same that are shown in Figure 1-right: There is a pump, evaporator, condenser, subcooler, accumulator and bypass line. Additional valving was added to facilitate operational flexibility and practical considerations such as leak checks, component removal and fill and drain procedures. Additional fittings were added to accommodate instrumentation; this included three Coriolis flow meters, three resistance temperature sensors and two thermocouples, a sight glass, one analog pressure gauge and six pressure transducers.

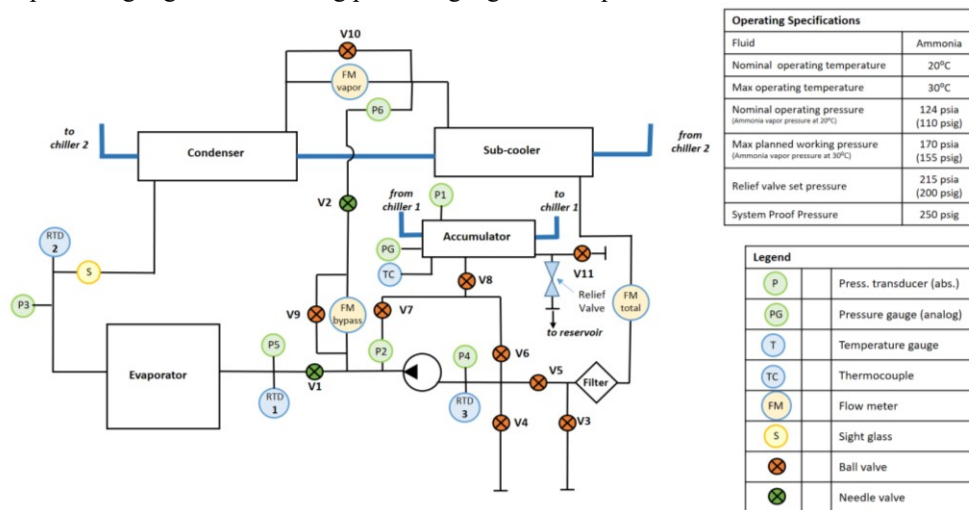


Figure 3. Schematic of Testbed. The primary functional components are the pump, evaporator, condenser, sub-cooler, and accumulator. The majority of the valving shown was used to facilitate testing, and is not necessary for system operation.

Liquid-Liquid plate heat exchangers were used for the condenser, subcooler and accumulator (Carlson Heat Exchanger – Model HP 316L 2.0 ST). A custom AM evaporator was used (details below). The pump was a miniature centrifugal pump (TCS Micropumps Ltd. – Model M510) that was modified for use with ammonia. All valves were diaphragm style (Swagelok – Model SS-4BK) except for two needle valves (Swagelok – Model SS-4BMRG) located at the inlet of the evaporator and in the bypass line. These were used to simulate varying line resistances. The accumulator was designed to be the high point of the system to ensure proper phase management during operation. All transfer lines were fabricated out of seamless 6.35 mm (0.25 in) 316 stainless steel tubing with 0.89 mm (0.035 in) wall thickness. Swagelok ferrule fittings and NPT fittings were used throughout the system. The RTDs were sheathed and installed to be in contact with the flowing fluid (Omega Engineering - Model PR-20); a type-E thermocouple was attached to the exterior of the accumulator to monitor its temperature. The coriolis flowmeters were calibrated for ammonia (BrokhorstUSA - Model M14), and valved bypass lines were incorporated around the flowmeters to provide the option of removing the flowmeters from the system flow path to lower the flow resistance. All pressure transducers were calibrated to read absolute pressure (Transducers Direct – Model TD1200). The sight glass was installed near the outlet of the evaporator (Rayotek – Model 101002). The analog pressure gauge (Ashcroft – Model 3967k51) was installed on the top of the accumulator. An infrared camera (FLIR) was used to image the evaporator temperatures. The entire system, except the top surface of the evaporator was

insulated. The condenser and subcooler temperatures were regulated using a single chiller, while the accumulator temperature was regulated using another chiller. A relief valve (Rego – Model SS9432T) vented to a water reservoir was incorporated for safety. Special care was taken to ensure that all materials used in the system were compatible with ammonia in order to obviate corrosion and the production of non-condensibles. The majority of the wetted materials were 316 stainless steel; the evaporator was made of an aluminum alloy (AlSi10Mg). Appropriate material selection and careful fill and drain procedures negated any concerns of non-condensable generation. The Max Allowable Working Pressure (MAWP) of the system was 1.38 MPa gauge pressure (200 psig). Heat loads were applied to the evaporator using three polyimide film heaters (Minco Products, Inc. – Model HAP). A photograph of the system prior to full insulation is shown in Figure 4.

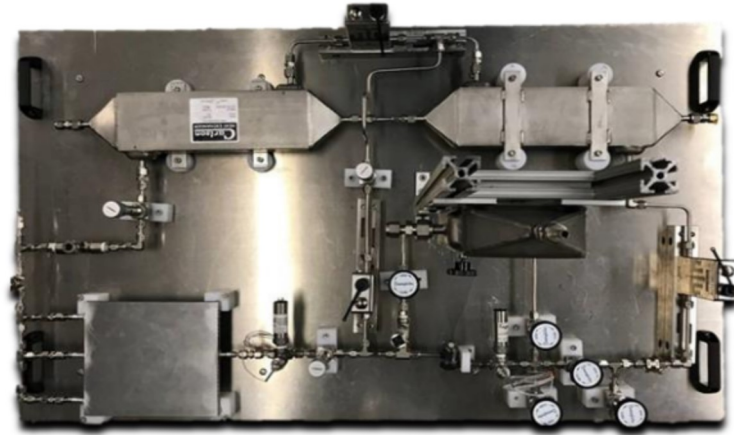


Figure 4. Photograph of the pump-assisted CPL. *This photograph was taken from above the testbed prior to insulation. The component layout follows the schematic shown in Figure 3.*

E. Evaporator Design

A novel monolithic AM planar evaporator was used in the system (Figure 5).^{10,11} The unit measured 213 mm x 198 mm x 16 mm (8.4 in x 7.8 in x 0.63 in) and had a mass of 1.3 kg. The general layout of the evaporator follows that of a CPL evaporator. The unit contained two flow channels (one for liquid and one for vapor) that were separated by a porous wick. However unlike a traditional CPL evaporator, the evaporator used here was fabricated as a single monolithic part using Direct Metal Laser Sintering (DMLS). Specialized machine settings were used to create porous and non-porous regions in the same part, in addition DMLS enabled the fabrication of complex geometries that would not be otherwise possible. This capability allows for CPL type evaporators to be fabricated with non-traditional geometries. Here, this technology has been used to fabricate a planar CPL-type evaporator.



Figure 5. The DMLS planar evaporator.¹⁰ *This monolithic evaporator combines integrated porous and solid structures. The general layout follows a CPL evaporator with the liquid and vapor channels separated by a wick.*

Figure 6 shows the internal details of the evaporator. The wick structure (blue) separates two networks of channels. One network of channels comprises the liquid side of the evaporator, while the other network of channels comprises the vapor side of the evaporator. This wick has a maximum pore radius of 22 μm , a permeability of $1\text{e-}13\text{ m}^2$, and a porosity of 24%. The evaporator contains solid pillars that connect the two planar faces to help withstand pressure. The unit was designed to withstand 250 psig. The array of holes were used to remove the residual powder from the evaporator after DMLS fabrication, and were subsequently welded shut. Three tubes were welded to the outlet of the evaporator to facilitate flow distribution; one tube was welded to the evaporator inlet.

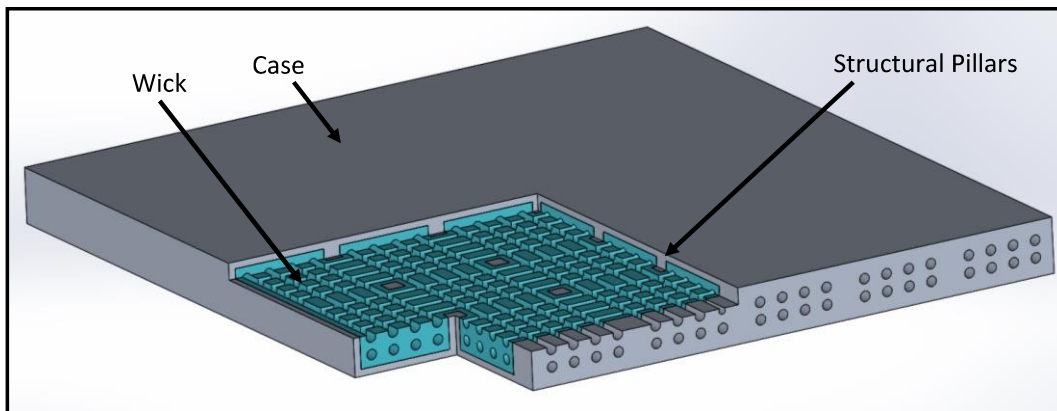


Figure 6. Evaporator internal structure.¹⁰ *The blue color is porous wick, while the gray color represents solid structure. The general architecture follows a CPL evaporator, where the liquid channels (bottom) are separated from the vapor channels (top) by a porous wick, and heat is applied at the top surface. Solid pillars connect the top and bottom of the evaporator planar faces to enhance structural support.*

IV. Testing

Once the pump-assisted CPL was fabricated and charged, an intensive test campaign was undertaken. The testbed was operated for a period of 350 hr over the course of 45 tests. Testing was done to verify that the architecture was working as expected and to explore the operating limits and start-up characteristics of the evaporator and system. The basic dynamics of the pump-assisted CPL (discussed in Section II-A) were confirmed for a wide range of operating parameters. Successful, stable operation was confirmed for heat loads ranging from 30 W to 850 W; heat fluxes ranging from 0.2 W/cm^2 to 13 W/cm^2 ; total system flowrates ranging 36 g/min to 208 g/min ; and liquid subcooling ranging from 5 $^{\circ}\text{C}$ to 10 $^{\circ}\text{C}$. For all tests, the accumulator was held at a constant temperature of 26 $^{\circ}\text{C}$ using an external chiller. The condenser and subcooler were held at 20 $^{\circ}\text{C}$ except when the subcooling was varied.

The nominal operating configuration consisted of a total system flowrate of 90 g/min, an accumulator temperature of 26 °C and a condenser and subcooler temperature of 20 °C. In this configuration the range of admissible heat loads that resulted in stable system operation was from 30 W to 325 W with a max allowable heat flux of 13 W/cm² (applied over a 14.2 cm x 1.3 cm area).

As was expected, it was found that the range of admissible heat loads that resulted in stable separated flow was a function of the mechanically pumped flowrate. As the flowrate increased, the maximum and minimum allowable heat load to produce separation of phases in the evaporator also increased. This behavior can be anticipated from the principles of operation outlined earlier in this paper and in Refs. 8,9. In addition it was also found that the maximum allowable heat load can be increased by increasing the fluid flow resistance in the bypass line. This was done by modulating the bypass line needle valve. This behavior again corroborates the principles of operation presented earlier in this paper and in Refs.^{8,9}

A. System Operation

For a typical system test, the following procedure was followed: (1) the accumulator was heated to 26 °C (ambient temperature was typically less than 20 °C) to bring the fluid in the primary loop to the subcooled condition; (2) the mechanical pump and condenser/subcooler chiller were turned on to begin to circulate fluid and isothermalize the fluid in the primary loop; (3) the bypass flowmeter calibration was checked by opening and closing specific valves; (4) the system was allowed to re-equilibrate to prepare for heat transport; (5) the evaporator heaters were turned on, resulting in vapor generation in the evaporator and vapor flow being established in the line connecting the evaporator and condenser; (6) the system was allowed to equilibrate to a steady state condition.

B. System Level Test Data

Figure 7 shows test data for heat loads between 50 W and 325 W at nominal operating conditions: the total system flowrate was 90 g/min, the accumulator temperature was 26 °C and the condenser and subcooler temperature were 20 °C. Both increasing and decreasing heat loads are shown. As is expected for the system, the evaporator outlet temperature is relatively constant and close to the accumulator temperature of 26 °C; it is only slightly affected by heat load (fluctuations less than ±0.5 °C). The pump inlet temperature is held fairly constant at 20 °C with the subcooler. Just prior to the application of the heat load (1.6 hr), the flowrate through the evaporator and bypass lines are approximately equal. This indicates that the single phase flow resistance through these lines are roughly equal. With the application of 100 W on the evaporator at start-up (1.6 hr) the flowrates through the evaporator can be seen to rapidly drop. This is due to the liquid-vapor interface becoming established in the evaporator wick which prevents the fluid from being forced into the evaporator by the mechanical pump (see Section II-A). The salient feature indicating that the system is working as anticipated, is that the flowrate through the evaporator increases as the heat load increases. This implies that capillary pumping is occurring in the evaporator, and that the liquid and vapor phases are appropriately separated. In a typical two-phase evaporator that does not incorporate capillary pumping (phase separation), the evaporator flowrate decreases as the heat load increases, due to the increase in pressure drop with increased quality. Indeed this was observed in present system when the heat load was below the minimum allowable heat load for stable separated flow operation (i.e. liquid was penetrating the wick and two-phase flow was present between the evaporator and condenser).

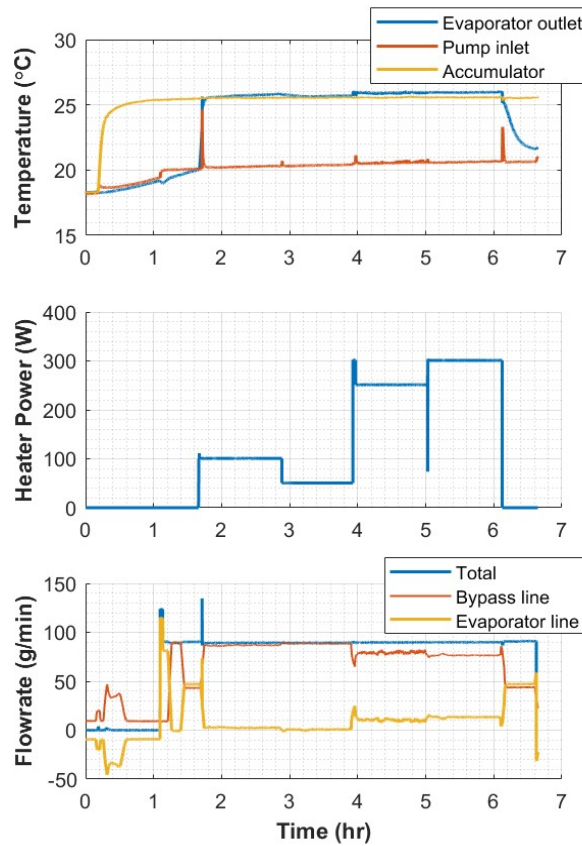


Figure 7. Test data from the two-phase MPFL. Representative data at nominal operating conditions (total system flowrate: 90 g/min; Accumulator temperature: 26 °C; condenser/subcooler temperature: 20 °C).

To further confirm that capillary pumping is indeed occurring in the pump-assisted CPL testbed, consider Figure 8. This plot shows the flowrate through the evaporator as a function of heat load for heat loads ranging from 30 W to 850 W and total system flowrates ranging from 36 g/min to 208 g/min. Superimposed on the data points is the ideal relation between mass flowrate and heat load assuming no losses (from an enthalpy including considering the latent heat of vaporization and subcooling). As can be seen the data falls very close to the theoretical values.

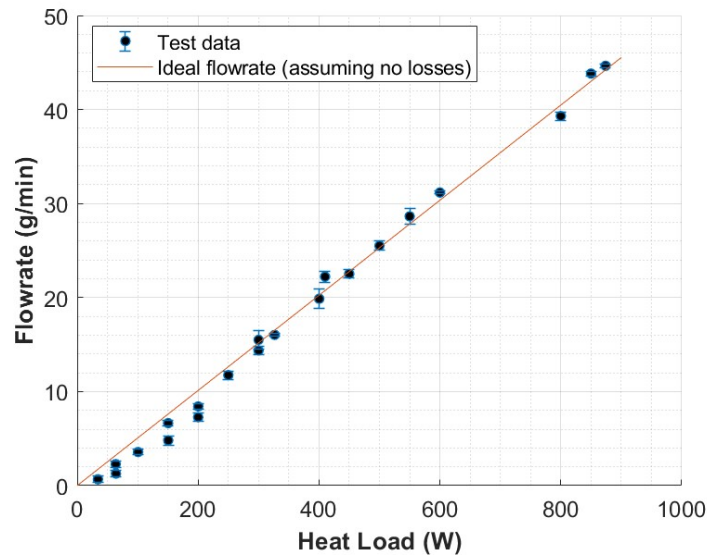


Figure 8. Evaporator mass flowrate as a function of heat load. *The data points show the relation of the evaporator mass flowrate versus flowrate; the line shows the ideal theoretical relation between these variables. The theoretical relationship was obtained by relating the mass flowrate to the heat load using the latent heat of vaporization, specific heat and degree of subcooling. Thermal losses from the heater were not accounted for in the theoretical calculation. The test data represents steady state system data collected over multiple tests.*

C. Evaporator Test Data

The data shown above demonstrate that the novel AM planar evaporator was able to sustain system level performance. However it is also of interest to look at the local performance of the evaporator, and in particular the degree of isothermality obtained during testing. The general trend was that for a given total system flowrate, when the heat load was not too close to the maximum allowable heat load, the evaporator was extremely isothermal. Figure 9 shows IR images of the evaporator for heat loads between 30 W and 325 W during nominal operation (total flowrate: 90 g/min; accumulator temperature 26 °C; condenser/subcooler temperature 20 °C). For 30 W and 100 W the temperature variation across the evaporator is less than 0.5 °C. For 150 W and 325 W most of the plate is similarly isothermal, however there are hot spots near the evaporator outlet that are about 3 °C warmer than the rest of the plate. In general, for a given pump speed, as the heat load or heat flux was increased, the isothermality was degraded.

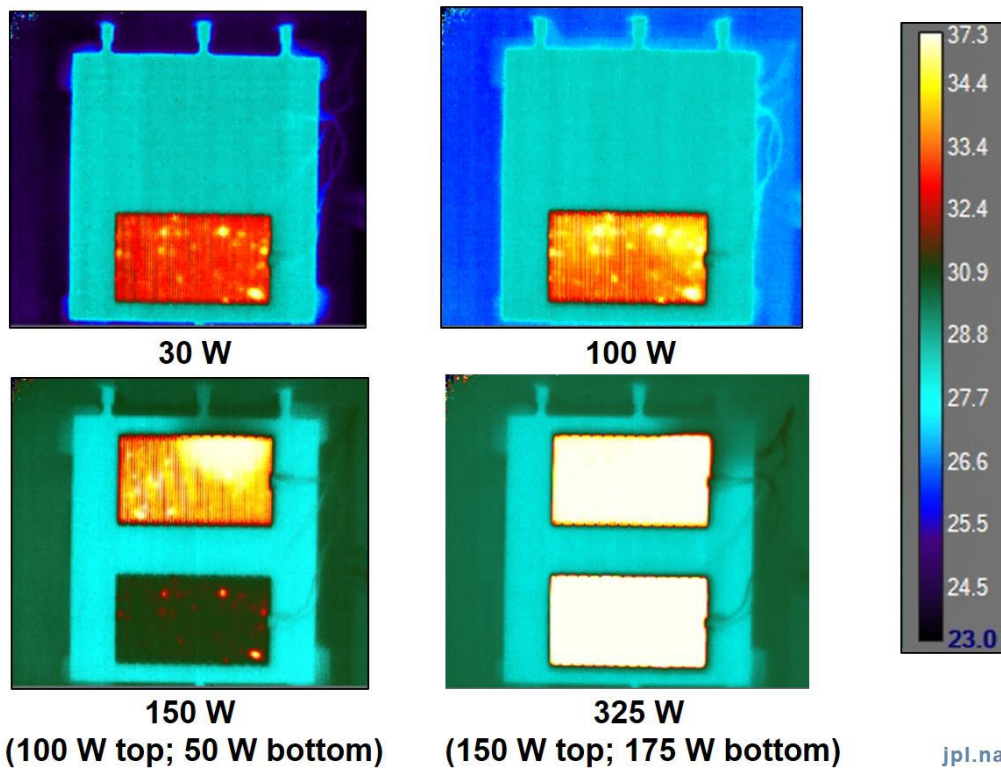


Figure 9. IR images of evaporator with applied heat loads. *The system is running at the nominal condition for all images conditions (total system flowrate: 90 g/min; Accumulator temperature: 26 C; condenser/subcooler temperature: 20 °C). Temperature excursions on the evaporator surface are less than 3 °C in all cases. For the lower heat loads (30 @ and 100 W) the temperature excursions are less than 05 °C. All heaters have the same*

V. Conclusion

A novel two-phase MPFL has been presented. The system architecture is a derivative a CPL, and can be described as a pump-assisted CPL. The system uses a CPL type evaporator layout and utilizes both capillary pumping within the evaporator as well as mechanical pumping. The operating principles of the system were described and preliminary test data was shown for an ammonia testbed. The testbed was shown to have stable performance for heat loads ranging from 30 W to 850 W, with heat fluxes up to 13 W/cm².

In addition an AM planar evaporator was presented and its performance was documented. The evaporator was shown to be able to maintain isothermality within 0.5 C for heat loads up to 100 W, and isothermality within 3 C for heat loads up to 325 W.

The two-phase MPFL system presented combines favorable attributes of both passive two-phase devices (CPLs/LHps) and single phase MPFLs. The favorable attributes are: (1) Maximum heat load and transport line length are not limited by the evaporator wick, but are a function of mechanical pump power; (2) Two-phase flow is minimized to only occur within the condenser—this makes the system more predictable and also reduces pump power requirements; (3) the system can incorporate mechanical fittings and valves as well as late routing changes to ease implementation; (4) the system can operate in adverse gravity fields by compensating for gravity head with the pump; (5) in case of pump failure the system can operate in a degraded performance mode as a CPL; (6) no pre-heating of the fluid is needed at the evaporator inlet to obtain an isothermal evaporator.

It is noted that including a mechanical pump in a spacecraft brings up concerns over the reliability of such a component. However, it has been demonstrated that with a judicious design, a centrifugal-style mechanical pump

can be robust and have a lifetime in excess of 12 years.* While this data point does not invalidate reliability concerns, it certainly indicates that they can be overcome.

Future plans for the current system include further testing and optimization, as well as the integration of flight-like components into a system level testbed. Flight opportunities for the technology are being actively sought.

Acknowledgments

This research was carried out at the Jet Propulsion Laboratory, California Institute of Technology, under a contract with the National Aeronautics and Space Administration. The authors would like to thank Gajanana Birur, for his technical advice and guidance and Subbarao Sarumpudi for his support of the project. The authors gratefully acknowledge the support from the JPL Research and Technology Development office that provided the funding for this work.

References

¹Swanson, Theodore D., and Gajanana C. Birur. "NASA thermal control technologies for robotic spacecraft." *Applied thermal engineering* 23.9 (2003): 1055-1065.

²Ponnappan, Rengasamy, Brian Donovan, and Louis Chow. "High-power thermal management issues in space-based systems." *AIP Conference Proceedings*. Vol. 608. No. 1. AIP, 2002.

³Spergel, D., et al. "Wide-field infrared survey telescope-astronomy focused telescope assets wfirst-afta 2015 report." *arXiv preprint arXiv:1503.03757* (2015).

⁴Sunada, Eric, et al. "A two-phase mechanically pumped fluid loop for thermal control of deep space science missions." *46th International Conference on Environmental Systems*, 2016.

⁵Zhang, Ping, Xianmeng Wei, Lipei Yan, Hui Xu, and Tao Yang. "Review of recent developments on pump-assisted two-phase flow cooling technology." *Applied Thermal Engineering* (2019).

⁶Ku, Jentung, and Edward J. Krolczek. *The Hybrid Capillary Pumped Loop*. No. 881083. SAE Technical Paper, 1988.

⁷Wrenn, Kimberly R., and David A. Wolf. "Test results for a high power thermal management system." *AIP Conference Proceedings*. Vol. 969. No. 1. AIP, 2008.

⁸Furst, Benjamin, Sunada, E., Cappucci, S., Bhandari, P., Daimaru, T., & Nagai, H. (2017, July). "A Comparison of System Architectures for a Mechanically Pumped Two-Phase Thermal Control System." *47th International Conference on Environmental Systems*, 2017.

⁹Cappucci, Stefano, et al. "Working Fluid Trade Study for a Two-Phase Mechanically Pumped Loop Thermal Control System." *48th International Conference on Environmental Systems*, 2018.

¹⁰Furst, Benjamin, Cappucci, S., Daimaru, T., Sunada, E., Roberts, S., & O'Donnell, T. (2018, July). "An Additively Manufactured Evaporator with Integrated Porous Structures for Two-Phase Thermal Control." *48th International Conference on Environmental Systems*, 2018.

¹¹Daimaru, Takuro, Furst, B., Cappucci, S., Sunada, E., Birur, G. "Development of an Evaporator Using Porous Wick Structure for a Two-Phase Mechanically Pumped Fluid Loop." *49th International Conference on Environmental Systems*, 2019.

¹²Ku, Jentung. "Thermodynamic aspects of capillary pumped loop operation." *6th Joint Thermophysics and Heat Transfer Conference*. 1994.

* A replica of the pump used on the Mars Pathfinder mission has been operating for over 12 years in a JPL pump lifetime test. The mechanical pump on the Mars Science Lab rover has been operating for over 7 years.